Potential Of Copper-Based MOFs As Heterogeneous Catalysts In Biodiesel Production From Waste Cooking Oil (WCO)

Nila Tanyela Berghuis[1], Fandry Hosea Jaby[2], Muttaqin[3*]

(nila.tanyela@universitaspertamina.ac.id[1], fandryjaby25@gmail.com[2], muttaqin@universitaspertamina.ac.id[3])

Department of Chemistry, Universitas Pertamina, South Grogol, Kebayoran Lama, Jakarta, Indonesia 12220 [1,2,3]

Abstract. Biodiesel is an alternative renewable energy source that is envisioned to be the most promising solution to fossil fuel dependency. Biodiesel can be manufactured from waste cooking oil with the assistance of MOF (Metal Organic Framework) based catalysts. This work involves the application of modified copper-based MOF-74 and HKUST-1 biodiesel synthesis. A series of analyses support that the Cu(II)-MOF framework was successfully formed with high yield 85% and it has moderate thermal resistance performance at 250°C. The effectiveness of two catalysts was evaluated, employing quantitative analysis to measure free fatty acid (FFA) levels and qualitative analysis using gas chromatography. As a result, the HKUST-1 catalyst performs well in both aspects, exhibiting the most substantial reduction in FFA from 12.28% to 7.46%. Furthermore, the HKUST-1 catalyst displayed consistent performance, with an average biodiesel yield remaining 80 percent. This results demonstrates the promising applicability of copper-based catalysts in the biodiesel synthesis process.

Keywords: Biodiesel, Heterogeneous catalyst, MOF-74, Waste cooking oil.

1 Introduction

Biodiesel is an alternative fuel to fossil fuels and is regarded as renewable option due to Biodiesel was established as a renewable fuel due to abundance of resources on the earth. The utilization of biodiesel as a fuel is currently still in the form of a mixture of diesel oil with a certain composition, although some use 100% biodiesel [1]. Chemically, biodiesel is composed of 16 to 20 carbon bonds with one, two, or no double bonds. Biodiesel has a methyl ester group ($R\text{-}COOCH_3$) at one end. The presence of oxygen-containing ester groups limits the use of biodiesel for any vehicle engine, because as an oxidizing accent, oxygen will make the combustion engine susceptible to corrosion. This is the reason why biodiesel as a fuel is generally mixed with diesel oil to suppress the corrosion rate of the engine. Scientists have optimized biodiesel with several types of chemical reactions to remove oxygen. However, these optimizations require particular reaction conditions, making them inefficient on an industrial

RESILIENCE 2023, November 24, Jakarta, Indonesia

DOI 10.4108/eai.24-11-2023.2346497

scale. Commercial biodiesel production techniques would be more suitable through catalyst-assisted biodiesel synthesis.

The catalyst commonly used in synthesizing biodiesel is homogeneous. Homogeneous catalysts are defined as catalysts that have the same phase as the reactants. The employment of homogeneous catalysts in biodiesel synthesis encounters some challenges. These challenges include complicated catalyst recovery, requiring additional separation techniques between catalyst products. In addition, the use of homogeneous catalysts results in low thermal strength at temperatures <250°C, prone to impurities, not to mention the catalyst neutralization process which requires a lot of water solvents, thus increasing operational costs [2]. Therefore, biodiesel synthesis using heterogeneous catalysts is gaining more attention due to its advantages over homogeneous catalysts. These include being easy to separate with simple separation techniques, economical, environmentally friendly, non-corrosive, and can be regenerated for reuse [3],[4]. Most heterogeneous catalysts use transition metal derivatives. Transition metals were chosen because they give the catalyst the Lewis acid properties necessary in biodiesel synthesis. Of the many types of heterogeneous catalysts that exist, MOF is a material that has recently received a lot of attention in the field of catalysts [5].

The principle involves interaction on the active side of the catalyst by utilizing pore stability and surface area [6]. As a heterogeneous catalyst, MOF can answer the weaknesses possessed by homogeneous catalysts in general. MOF is capable of fulfilling the specificity, selectivity, and chirality aspects of catalyst materials for various types of reactions, one of which is for biodiesel synthesis [7]. In addition, MOF has other advantages such as ease of separation technique at the end of the reaction, better mechanical strength, cost-effectiveness, and can be regenerated for reuse. Another uniqueness of MOF is that it can be modified, either by changing the type of transition metal or ligand or by inserting a support into the MOF matrix to obtain MOF with stronger mechanical and thermal resistance [8]. In this research, the types of MOF used are MOF-74, Cu-BDC, and Cu-BTC (HKUST-1) based on copper metal Cu(II). The three types of MOF have been widely studied as adsorbents and separators for small molecules. Furthermore, MOFs also provide many active sides that act as Lewis acid species. A number of these advantages are interesting studies to be analyzed regarding the potential of Cu(II) metal-based MOFs as heterogeneous catalysts in the biodiesel synthesis process.

2 Experimental Section

2.1 Materials

The chemicals used during the research included copper(II) nitrate trihydrate ($Cu(NO_3)_2 \cdot 3H_2O$ ≥99.5%, Merck KGaA), magnesium nitrate hexahydrate ($Mg(NO_3)_2 \cdot 6H_2O$ ≥99%, Merck KGaA), 2,5-dihyroxyterephtalate acid (H_4DOBDC 98%, Sigma-Aldrich), terephtalic acid (H_2BDC 99%, Sigma-Aldrich), trimesic acid (H_3BTC 95%, Sigma-Aldrich), N,N'-dimethylformamide (≥99.8%, Merck KGaA), n-hexane (98%, Merck KGaA), methanol (≥99.9%, Merck KGaA). Biodiesel synthesis using used cooking oil or WCO feedstock (pH around 5; density 0,897 g/cm^3).

2.2 Synthesis of MOF-74

The preparation of monometallic Cu-MOF-74 and bimetallic CuMg-MOF-74 samples follows the working procedure in the previous publication with some modifications in the working method [9],[10]. The monometal Cu-MOF-74 synthesis begins with the preparation of a solution of 2 mmol $Cu(NO_3)_2 \cdot 3H_2O$ in 10 grams of DMF and a solution of 1 mmol H_2DOBDC ligand in 10 grams of DMF separately. The ligand solution was added to the metal solution one drop at a time while stirring until homogeneous at room temperature for 20 hours. The suspension was then heated in an 80°C oven overnight, after which the suspension was allowed to cool at room temperature. MOF-74 solids were obtained by centrifugation at 6500 rpm for 10 minutes, where MOF-74 was washed using DMF twice and methanol three times. The wet MOF-74 was dried through oven heating at 80°C overnight. After that, MOF-74 was activated using a tubular furnace at 150°C for 5 hours in an argon gas atmosphere before being used for the catalysis stage.

The synthesis of CuMg-MOF-74 bimetal began by preparing a solution of 1 mmol H_2DOBDC ligand in 10 grams of DMF, 1 mmol $Cu(NO_3)_2 \cdot 3H_2O$ in 5 grams of DMF, and 1 mmol $Mg(NO_3)_2 \cdot 6H_2O$ in 5 grams of DMF. The ligand solution was added to the Cu(II) solution one drop at a time while stirring at room temperature until homogeneous. After one hour, magnesium solution was added dropwise to the Cu-DOBDC mixture. The bimetallic mixture was left to react for four days. To obtain the bimetallic catalyst, the same method was used as the previous monometallic catalyst, namely centrifugation. Then CuMg-MOF-74 was dried and activated at 150°C for 5 hours in an argon gas atmosphere before being used for catalysis.

2.3 Synthesis of HKUST-1

The synthesis method of both Cu-BDC and Cu-BTC variations commenced with the preparation of each precursor, including 5 mmol of $Cu(NO_3)_2 \cdot 3H_2O$ salt and 5 mmol of each ligand. Both reagents were put together in a Duran bottle and dissolved in 50 mL of DMF. Once the solution was fully homogenized, it was heated in an oven at 120°C for 36 hours. The catalyst suspension was allowed to settle down at room temperature for some time. After it cooled down, the catalyst was obtained by centrifugation technique at 6500 rpm for 10 minutes, then washed with methanol three times. The wet catalysts were then dried by heating in an oven at 80°C overnight. After drying, Cu-BDC and Cu-BTC were activated using a furnace at 160°C with argon gas. The activated Cu-BDC and Cu-BTC can then be used as catalysts for biodiesel synthesis.

2.4 MOF Characterization

Infrared absorption analysis was performed using a Thermo Scientific NICOLET iS5 instrument at wavelengths of 400-4000 cm^{-1}. IR radiation came from a high-intensity halogen NIR diode source. The FTIR testing technique was performed based on KBr plates. The crystal size and crystallinity of MOF catalysts were determined based on X-ray diffractograms using a PANalytical Aeris XRD Benchtop instrument with a Cu-Kα radiation source (λ = 1.5406 Å) of 40 kV. Surface attributes at the microscopic scale can be seen through SEM analysis using an FEI Quanta QEMSCAN 200 instrument under vacuum conditions up to 20 Torr with Bruker 30

mm^2 twin dispersion energy spectroscopy. Thermal strength testing of MOF catalysts was tested using TGA Discovery TA SDT650 in the temperature range of 30-600°C. The instrument was set at a heating rate of 20°C/minute in a nitrogen gas atmosphere.

2.5 Biodiesel Synthesis using MOF Catalyst

The activated catalysts were tested for their ability to synthesize biodiesel according to published procedures [11].[12]. Some 10 grams of WCO was prepared in a round bottom flask attached to a reflux system. The used cooking oil was then combined with methanol at a methanol: oil ratio of 10:1. Then, about 0.08 grams of MOF-based catalyst was added to the mixture of oil and methanol. The system was reacted at 60°C for 5 hours. When the reaction was complete, the MOF catalyst and biodiesel were separated by centrifugation while being washed using n-hexane. Then, the biodiesel was separated again from glycerol and other residuals by washing it with 50 mL of n-hexane in a separating funnel. The biodiesel phase is stored in a container to be heated at 70°C so that all solvents are removed/evaporated. The biodiesel was then ready for analysis.

2.6 Biodiesel Characterization

WCO samples, as well as other biodiesel products, were analyzed using gas chromatography in tandem with mass spectrometry (GC-MS) Thermo Scientific Trace 1310. The chromatography column used was TG-5-MS with dimensions of 30 m x 0.25 mm x 0.25 μm. The oven temperature was set at 70°C for 5 minutes until 270°C was maintained for 15 minutes with a ramp of 25°C/minute. Helium gas with a flow rate of 2 mL/min was introduced as a carrier gas. The test mode was split mode with a ratio of 20:1. The amount of sample tested was 1 μL through the injector port with a temperature of 200°C. For tandem MS using an ion source with a temperature of 200°C with a detection of 30-400 amu.

3 Results and Discussion

The overall research has successfully synthesized four variations of MOF catalysts. Two of them are MOF-74 groups with monometal Cu-MOF-74 and bimetal CuMg-MOF-74 modifications, while the other two catalysts are Cu(II) metal-based MOFs with modifications to the ligands, which are BDC and BTC. The four MOFs will be used as acid catalysts in the synthesis of biodiesel from WCO feedstock. These four MOF catalyst samples were all synthesized using the organic solvent medium DMF. DMF can dissolve the metal ions and ligands used because it has similar polarity as well as intermolecular force properties towards the solute [13]. Considering its molecular structure, DMF has nitrogen and oxygen atoms with high electronegativity. These atoms have a strong tendency to attract positively charged ions such as protons. Oxygen atoms have a greater electronegativity than nitrogen atoms, so protons will be attracted by oxygen atoms. The alkaline nature of DMF is also described by the formation of hydroxy ions (OH^-) according to the Arrhenius concept.

MOF synthesis generally uses basic solvent media such as DMF, DEF (N, N'-diethyl formamide), DMSO (dimethylsulfoxide), methanol, or ethanol [14]. This alkaline nature is required to deprotonate or release hydrogen atoms on organic ligands. This deprotonation causes

the ligand to become negatively charged, so it can interact with positively charged metal ions. The other properties of the solvent used as a modulator agent. This modulator agent is generally owned by solvents that have nitrogen atoms [15]. The presence of this modulator property is considered important to boost the nucleation rate of MOF crystals and achieve high crystallinity [16]. Nucleation is an atomic-scale thermodynamic process of growing nuclei or particles into new, more stable structures. There are two types of nucleation: homogeneous and heterogeneous nucleation. Homogeneous nucleation occurs in the system itself remote from the surface of the suspension (nucleation starts from the inner wall of the container), while heterogeneous nucleation is caused by external triggers that promote crystal growth [17], [18]. Therefore, with the help of heat triggers the kinetics of metal particles and ligands to coordinate with each other until finally forming MOF crystals.

Table 1. Total Mass of the Synthesized MOF-74

Catalyst	$Cu(NO_3)_2 \cdot 3H_2O$	$Mg(NO_3)_2 \cdot 6H_2O$	H_4DOBDC	DMF	Total Mass
Cu-MOF-74	1,467 g	---	0,598 g	65 mL	0,669 g
CuMg-MOF-74	0,750 g	0,771 g	0,597 g	67 mL	0,603 g

Table 2. Total Mass of the Synthesized HKUST-1

Catalyst	$Cu(NO_3)_2 \cdot 3H_2O$	H_2BDC	H_3BTC	DMF	Total Mass
Cu-BDC	1,241 g	0,861 g	---	50 mL	1,833 g
Cu-BTC	1,245 g	---	1,102 g	50 mL	1,301 g

In this study, MOF catalysts were used because they have certain advantages over other types of heterogeneous catalysts, such as natural/native heterogeneous catalysts. These catalysts are naturally found in the form of oxide solids. Before use, oxide catalysts are necessary to be activated to increase the reactivity and surface area of the catalyst. The modifications of these oxide catalysts are quite difficult to do due to their complex and rigid structure [19]. In addition, natural catalysts undergo an evolutionary process to assist a specific reaction, so they cannot be applied to various chemical reactions in general. To overcome the limitations of natural catalysts, MOF catalysts promise to be flexible and can be modified according to the needs of the reaction [20],[21]. The composition of metals and ligands as precursors as well as the synthesis method can be changed to optimize the physical properties of MOFs. From the aspect of porosity, MOF can provide a larger surface area so that the reaction occurs more effectively [22]. Since they are easily modified, MOF applications can be undertaken in various types of reactions, including biodiesel synthesis.

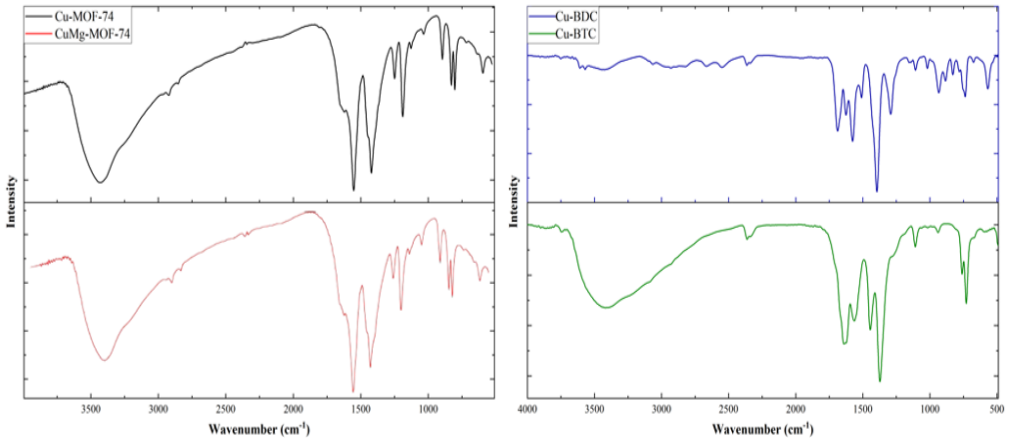

Fig. 1. Infrared spectra of MOF-74 (left) and HKUST-1 (right)

MOF analysis using FTIR was conducted to acquire qualitative outcomes shown in **Figure 1.** above. The qualitative test results are the distribution of IR absorption spectra in the fingerprint area at the wavenumber approximately <1000 cm^{-1}. Infrared absorption results successfully identified the bonding of Cu(II) metal with 2,5-dihydroxyterephthalate ligand at a wavelength of 803 cm^{-1} for both monometallic and bimetallic MOF-74 samples. On the other hand, the spectrum of CuMg-MOF-74 gives an absorption of 1035 cm^{-1} indicating the delocalization of electrons of the -COO- group. This delocalization is induced by the difference in electronegativity between Cu and Mg metal [23]. Meanwhile, Cu(II) and ligand metal bonds for HKUST-1 were identified at wave numbers 737 cm^{-1} for Cu-BDC and 729 cm^{-1} for Cu-BTC [24]. This region is a distinct area of organometallic bonds, which is a compound formed between a metal center atom and an organic compound. Other areas indicate intermolecular bonds in organic compounds. For example, the sharp spectra at wave numbers around 1500 cm^{-1} and 1200 cm^{-1} are typical for -C=O and -C-O- bonds from the carboxylic group of the utilized ligand. There is certainly a chemical shift when compared to theoretical values. This shift is influenced by the interaction of ligand molecules with the metal center[25]. The absorption detected in the area around 3420 cm^{-1} which shows the hydroxyl functional group (-O-H). This absorption is most likely caused by the presence of residual moisture in the form of water molecules (H_2O) attached to the MOF framework. By comparing the IR spectra in **Figure 1.** to other research that has been conducted beforehand, the synthesis of MOF-74 and HKUST-1 shows the interaction of the Cu(II) metal center and each ligand in the range of 720-800 cm^{-1}. These spectra also confirm the coordination between Cu metal and the ligand that builds the MOF matrix. The spectra of other bonds such as C-O and C=O in carboxylic groups as well as C-C, C=C, and C-H bonds in benzene experienced changes or shifts in wavenumber values and intensity as well as peak shape. The chemical shift is very reasonable when there are differences in the metal centers and ligands used [26]. By comparing the IR spectra of the synthesized results to the references, the bond between Cu(II) metal and its ligand for each catalyst has been formed.

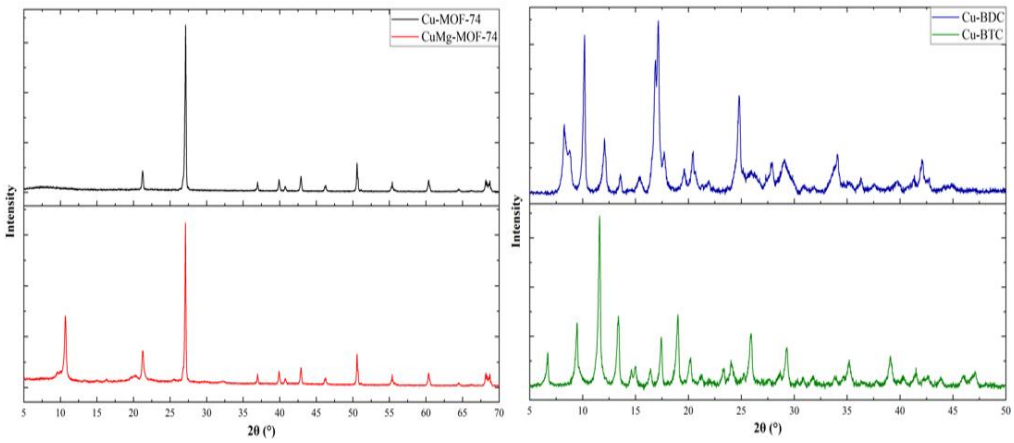

Fig. 2. X-Ray diffraction patterns of MOF-74 (left) and HKUST-1 (right)

Analysis of XRD data obtained in the form of diffractograms of spectral peaks at 2θ values in correspondence with Bragg's law. The sharp peaks indicate the crystal phase used to determine the crystal size as well as the percentage of crystallinity of the MOF obtained. Based on XRD pattern in **Figure 2.**, he diffractogram results for monometallic Cu-MOF-74 produced crystallite peaks at 2θ of the following 21,25°; 27,12°; 36,98°; 39,9°, 42,92°, 50,57°, 55,37°; dan 60,37°. Then for the bimetallic CuMg-MOF-74 produces a 2θ peak similar to the previous peak, which are 10,69°; 21,25°; 27,09°; 36,98°; 39,9°; 42,92°; 50,57°; 55,37°; dan 60,37°. The crystal peaks that appear comply with the research related to MOF-74 that has been conducted [10], [25]. The diffractogram shown for the HKUST-1 catalyst shows Cu-BDC crystallite peaks at 8,28°; 10,18°; 12,06°; 17,16°; 20,42°, dan 24,78°. Meanwhile for Cu-BTC, the values of 2θ are 6,70°; 9,48°; 11,60°; 13,38°; 17,44°; 19,00°; 25,92°; dan 29,32° [24], [27]. Crystallinity is the degree of structural order in a unit cell for a crystal lattice. The more organized, the higher the crystallinity of a material. XRD data can determine the crystallinity of the catalyst with the help of Origin2023 software. Crystallinity is determined by measuring the ratio of crystal peak area to total area on the diffractogram. The crystallinity of Cu-MOF-74 and CuMg-MOF-74 catalysts were 85.34% and 89.64%. While the crystallinity of Cu-BDC and Cu-BTC catalysts was 91.50% and 90.47%, respectively.

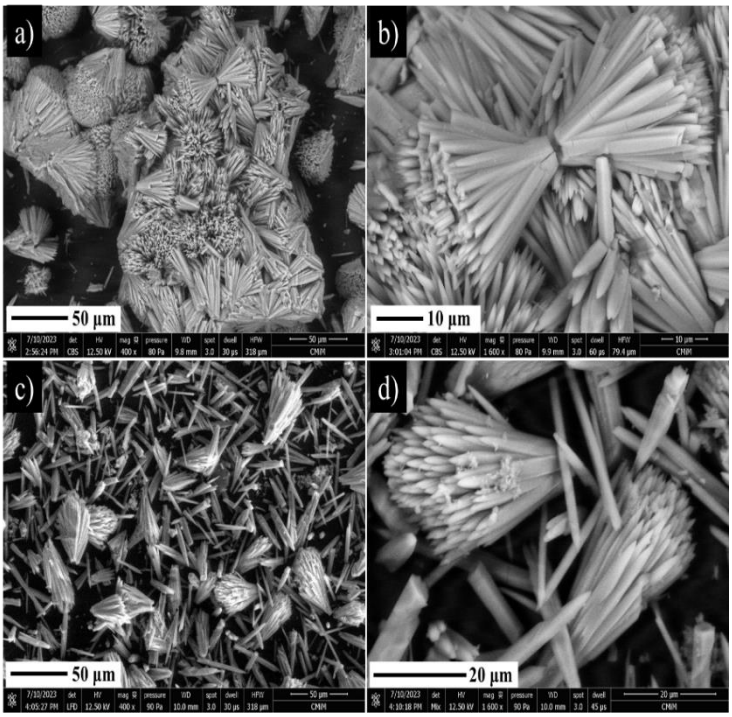

Fig. 3. SEM image of MOF-74

SEM images for both MOF-74 in **Figure 3.** above display similar crystal structures of needle-like shape. However, at smaller magnifications, there are characteristic differences. Cu-MOF-74 crystals are seen clustered together to form larger chunks. Meanwhile, CuMg-MOF-74 crystals are randomly distributed among each other, whether they are smaller or larger crystals. As opposed to MOF-74, HKUST-1 crystals in **Figure 4.** are shaped like chunks varying in size. The SEM analysis results for both catalysts above follow the crystallite size values of the catalysts in the previous XRD analysis. MOF-74 catalyst has a larger crystallite size than HKUST-1 catalyst [28,29], [15].

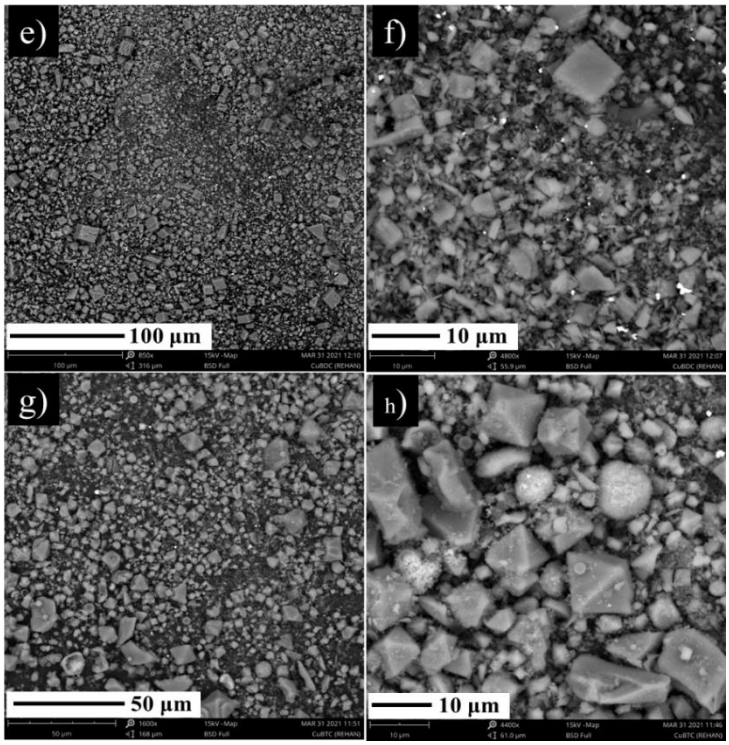

Fig. 4. SEM images of HKUST-1

Thermal strength assessment of MOF catalysts generated data in the form of thermograms shown in **Figure 5.** measuring the change in sample mass concerning temperature increase. Based on the thermogram below, the monometallic Cu-MOF-74 catalyst experienced one reduction in mass percentage at 284.24°C, while the bimetallic CuMg-MOF-74 decreased twice at 84.58°C and 277.4°C. The first change is a stage of detachment of water or any molecules from the MOF, then the second change is caused by the decomposition of organic compounds from the MOF. This demonstrates the hygroscopic nature of CuMg-MOF-74 or its ability to absorb moisture. Consequently, the presence of Mg(II) metal tends to increase the sensitivity of MOF-74 to water molecules in the open air. Such sensitivity underlies the application of Mg(II)-based MOF-74 as an excellent adsorbent material for smaller molecules such as CO_2, water, and methane [30], [31], as well as heavy metals which are environmentally poisonous [32]. As for the HKUST-1 catalyst, the Cu-BDC catalyst has better thermal resistance than Cu-BTC. Cu-BDC catalyst undergoes two gradual degradations at 263.95°C and 418.21°C. The thermograms of Cu-BTC catalyst shows a distinct degradation trend from the previous three types of catalysts. Similar to CuMg-MOF-74 bimetallic catalyst, Cu-BTC catalyst also has hygroscopic properties. The higher the temperature, the Cu-BTC thermogram continues to experience more changes in the Cu-BTC thermogram slope which indicates the instability of the Cu-BTC catalyst, especially at temperatures >150°C. In the end, the graph changes drastically and decays at a temperature of 349.61°C.

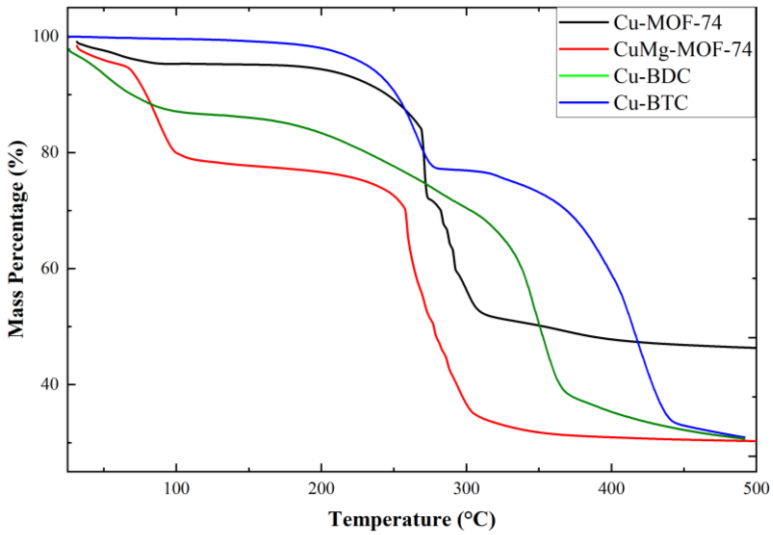

Fig. 5. Thermal analysis (TGA) of all Cu(II)-based MOF

Examination of the thermal properties for MOF-74 has also been carried out by previous publications which show the resistance of magnesium-based MOF-74 is weaker than copper-based MOF-74 [23]. This can be seen from the thermogram of CuMg-MOF-74 produces a fairly sharp gradient/slope of the mass percentage reduction curve. In contrast, the presence of Cu(II) metal improves the thermal resistance of MOF-74. The thermogram performance of Cu-MOF-74 shows much better resistance and the mass change is not as significant as that of CuMg-MOF-74.The thermogram demonstrates that at elevated temperatures up to 600°C, more Cu-MOF-74 samples can survive than other catalysts. Despite the addition or substitution of the central metal with transition metals carried out in this study, MOF-74 which is susceptible to moisture can be further modified to change its hydrophilicity. Several methods have been made such as functionalization of MOF-74 with other organic groups, coating or composite treatment, different synthesis methods, as well as doping techniques to add support to the MOF-74 matrix [33] The robustness difference between Cu-BDC and Cu-BTC is driven by the divalent Cu(II) metal interaction between the dicarboxylate ligand and the tricarboxylate ligand. The dicarboxylate ligand (BDC^{2-}) has an equivalent charge to Cu(II) metal of two, while the tricarboxylate ligand (BTC^{3-}) has a three-valence charge. The difference in charge will have an impact on the bonding arrangement of the HKUST-1 material [26]. This is why the thermal resistance of Cu-BDC catalyst is more stable than Cu-BTC catalyst.

As in the previous method, the synthesis of WCO into biodiesel involves alcohol and the role of catalysts. The synthesis takes place in a reflux system. Reflux is the most common synthesis method when volatile solvents are included. A solvent is said to be volatile if it has a boiling point far below the boiling point of water. Reflux is assisted by heating at temperatures close to the solvent's boiling point. To inhibit the solvent from evaporating and leaving the reaction, a condenser is installed. The way the condenser works is by cooling the solvent at the vapor phase back down to its liquid state. Another purpose of the condenser is to minimize the

vapor pressure in the reflux system. Biodiesel catalysis was carried out using the four types of catalysts that had been synthesized in the initial procedure. Each catalyst was regenerated for reusability in three recycles. In the end, a total of 12 biodiesel samples were collected. The biodiesel samples were named according to the type of catalyst used and the number of cycles used. Biodiesel from the synthesis with Cu-BDC, Cu-BTC, Cu-MOF-74, and CuMg-MOF-74 catalysts in the first cycle were labeled Biodiesel 1A, 2A, 3A, and 4A, respectively. Then in the second cycle, they were labeled Biodiesel 1B, 2B, 3B, and 4B. Finally, the third cycle was labeled Biodiesel 1C, 2C, 3C, and 4C. Biodiesel synthesis using MOF-based heterogeneous catalysts happens by utilizing the center atom of Cu(II) as a Lewis acid. Lewis acids are species that act as acceptors or recipients of free electron pairs. Cu(II) metal has vacant d orbitals so that hydrocarbon molecules – fatty acids and triglycerides in this study – can attach to Cu(II) metal and carry out the synthesis reaction into biodiesel [34]. The mechanism of fatty acid conversion by esterification with MOF catalyst in **Figure 6.** below.

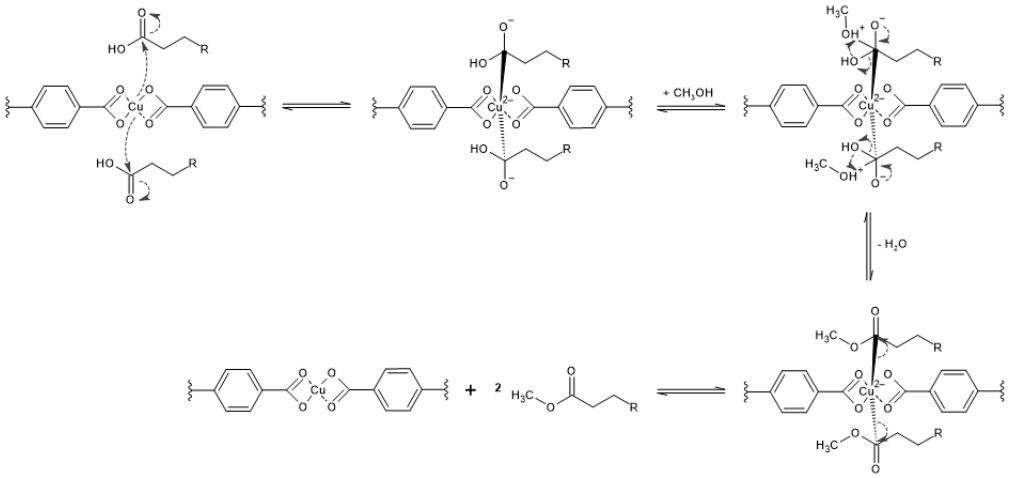

Fig. 6. Mechanism of fatty acid esterification reaction using Cu-MOF catalysts

The reaction mechanism of biodiesel synthesis over Cu(II) metal center above illustrates the coordinated system between Cu(II) metal, ligand, and two fatty acid molecules forming an octahedral structure. This is because the electron configuration of Cu(II) produces a d-count of d^9, meaning that there are 9 electrons in the d orbital. This circumstance causes Cu(II) metal to be able to use all available electrons to bind or interact with other molecules. The Cu(II)-MOF and fatty acid complex forms an octahedral since this structure is the most stable, and orbital overlapping occurs to the maximum extent to strengthen the bond with minimum intramolecular repulsion [33], [35]. Triglyceride molecules also undergo the same stages of synthesis as fatty acid molecules shown in **Figure 7.**, but they are sterically larger due to the larger size of triglyceride molecules than fatty acid. Triglycerides undergo a three-step synthesis because they have three ester branches that will be modified according to the following mechanism. After the ester part containing alkyl R^1 has been transesterified, the resulting by-product will bind back to the Cu(II)-MOF metal center. Esters containing R^2 and R^3 alkyls will be converted into methyl esters and glycerol will appear as the side product.

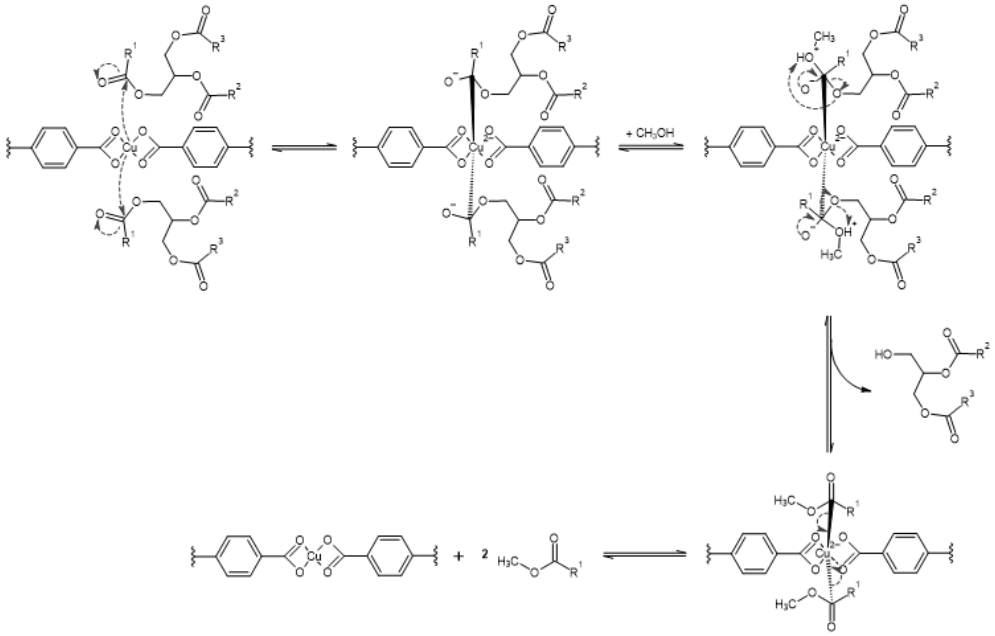

Fig. 7. Mechanism of triglyceride transesterification reaction using Cu-MOF catalysts

The WCO feedstock and the catalyzed biodiesel were analyzed using quantitative and qualitative approaches. The quantitative analysis of the oil employed was the determination of FFA (free fatty acid) concentration using the titration method with NaOH solution. For qualitative analysis, the samples were tested by GC-MS characterization. Determination of FFA content was carried out by titration method using 0.1 N NaOH solution and three drops of phenolphthalein indicator. The constituent component of WCO was assumed to be palmitic acid (256.42 $g \cdot mol^{-1}$).

Table 3. Comparison of WCO Mass to the Mass of Biodiesel Product

Sample	Average Weight	Average NaOH Volume	FFA Content
WCO	17,96 g	0,86 mL	12,278%
Biodiesel 1A	2,0075 g	0,06 mL	7,664%
Biodiesel 2A	2,0075 g	0,085 mL	10,857%
Biodiesel 3A	2,0275 g	0,085 mL	10,883%
Biodiesel 4A	2,020 g	0,075 mL	6,982%
Biodiesel 1B	2,062 g	0,06 mL	7,461%
Biodiesel 2B	2,0555 g	0,085 mL	10,604%
Biodiesel 3B	2,007 g	0,085 mL	10,86%
Biodiesel 4B	2,031 g	0,085 mL	10,732%
Biodiesel 1C	2,012 g	0,07 mL	8,921%
Biodiesel 2C	2,005 g	0,085 mL	10,871%
Biodiesel 3C	2,031 g	0,075 mL	9,469%
Biodiesel 4C	2,0185 g	0,085 mL	10,798%

Gas chromatography analysis is performed to separate the molecules, while mass spectrometry is used to identify the molecules that have been separated previously. The chromatogram shows the compounds that have successfully eluted and reached the detector. The detector will identify the type of compound that corresponds to the database on the computer-based on mass spectrometry analysis. The chromatogram shows the products of WCO catalysis using Cu-BDC and Cu-BTC. The analysis showed several products derived from ester compounds that constitute the biodiesel structure. According to **Figure 8.** of the chromatography analysis, Cu-BDC catalyst produced about 30.26%; of ester products while Cu-BTC catalyst produced 42.67%. Based on the chromatogram, the MOF-74 catalysis also produced some ester-derived products. Biodiesel catalysis using Cu-MOF-74 produced 26.53% ester compound products, while a total of 17.99% ester products were obtained from CuMg-MOF-74 catalysis.

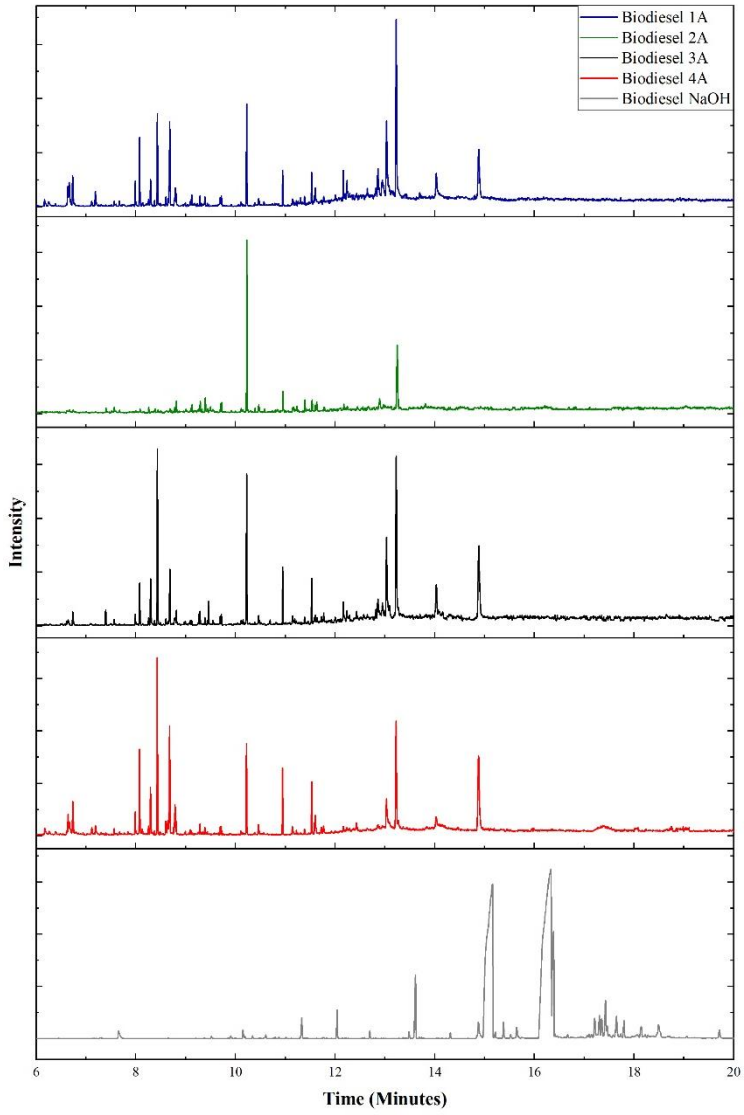

Fig. 8. Cromatography of biodiesel

Chromatographic analysis and identification of biodiesel synthesis products show a correlation between molecular shape and retention time. The greater the size of the hydrocarbon tends to have the longer the retention time [36]. This is because the longer chain size causes the molecule to have a stronger interaction with the chromatography column so that it is retained longer. This means that the chromatography column used has a similar polarity to the biodiesel molecules [37]. The GC results have shown the potential of copper-based MOF catalysts to be used in biodiesel synthesis. However, the percentage produced is not as good as biodiesel synthesis using homogeneous catalysts such as NaOH. The chromatogram results showed a

greater percentage of ester products at retention times between 12 to 17 minutes. GC results identified 29.99% of methyl hexadecanoate and 38.03% of methyl octadecanoate products and their derivatives, with 14.07% of other products being methyl esters and their derivatives with varying chain lengths ranging from C_7 to C_{15}. The total ester product obtained from biodiesel synthesis using NaOH catalyst was 79.52%. Methyl ester products from homogeneous catalysts can be greater based on other studies conducted [38], [39].

As shown in **Figure 8.**, each catalyst produces a varying percentage of biodiesel product which can be analyzed based on the interaction of each catalyst with the oil molecules. Both esterification and transesterification reactions are equilibrium reactions. The equilibrium of this reaction is dependent on several factors that determine the direction of equilibrium and the amount of biodiesel product produced. Based on the current study, the equilibrium and efficiency of biodiesel synthesis using MOF catalysts are strongly influenced by the presence of water. Water molecules can change the equilibrium direction of the esterification reaction by hydrolyzing ester compounds back into carboxylic acids. In addition, water molecules can bind coordinately with the Cu(II) metal center because water can behave as a ligand [40]. This can be explained by the hygroscopic nature of some MOF catalysts, including Cu-BTC and CuMg-MOF-74. Moreover, the biodiesel synthesis reaction is carried out at a temperature below the boiling point of water so that water molecules are not easily separated from the MOF frame. As such, the number of Cu(II) metal sites used to coordinate with oil molecules would be less than optimal. However, the HKUST-1 catalyst produced a greater percentage of biodiesel product than the MOF-74 catalyst due to its wider and more open surface. [41]. From SEM analysis, the MOF-74 crystals clustered together into a more compact structure and concealed the Cu(II) metal sites [42]. The blocked metal sites will increase the steric hindrance of MOF-74 catalyst, hence the biodiesel synthesis is not optimized when compared to HKUST-1 catalyst with a larger MOF surface.

The results of the synthesis using Cu(II)-based heterogeneous catalysts based on the chromatogram in **Figure 8.** tend to produce hydrocarbon fractions with smaller chain lengths. This can be seen by the appearance of peaks at a faster retention time than the chromatogram of biodiesel synthesis using NaOH catalyst. The reactions that occur include cracking of the carbon chain and the reaction of converting carboxylic groups into other functional groups. These reactions certainly change the physical properties of the compounds obtained such as the boiling point of the compounds [43]. Some compounds are likely to be lost during the washing and heating stages to obtain biodiesel after reflux. This situation can explain the mass of WCO lost after being synthesized into biodiesel in the previous table. The difference in mass of WCO and biodiesel (%w/w) is based on the assumption that all components in WCO are converted into biodiesel and no significant mass change occurs. The smaller hydrocarbon structure is potentially compatible with diesel fuel applications. Diesel is a mixture of hydrocarbon fractions with chain lengths between C_9 to C_{15} used as engine fuel such as gasoline and diesel [44].

Based on the comparison of the percentage of ester products between NaOH catalyst and copper-based MOF catalyst, the heterogeneous catalyst used still has limitations in terms of specificity and selectivity. In this study, the method used to see the improvement of MOF catalyst performance in biodiesel synthesis was to change the ratio of the amount of WCO to

the amount of catalyst. The analysis was done qualitatively by looking at the FFA content of the synthesized biodiesel. The amount of WCO used was 75% and 50% by mass, while the amount of catalyst and methanol were kept constant. As a result, the smaller the mass of WCO used, the smaller the FFA content. As before, the FFA content was determined by titration using 0.0645 N of NaOH solution.

Table 4. FFA Content for Synthesis of 75% and 50% Mass of WCO Used

Oil Content	Biodiesel Mass		NaOH Solution		Average FFA Content
	m_1	m_2	V_1	V_2	
75% WCO	3,021 gr	3,004 gr	0,13 mL	0,13 mL	5,49%
50% WCO	2,016 gr	2,013 gr	0,06 mL	0,06 mL	4,826%

Increasing the effectiveness of methyl ester synthesis can also be done by utilizing catalyst reproducibility for three cycles of the same catalyst. Each percentage of methyl ester product identified by GC analysis for each cycle was summed according to the data in Table 5 below. The results showed that biodiesel synthesis using HKUST-1 catalyst for three cycles gave a better product percentage than using NaOH catalyst. This is also in accordance with other studies that used HKUST-1 catalyst for biodiesel synthesis.

Table 5. Percentage of Methyl Ester Products After Three Cycles of Synthesis

Catalyst	Percentage of Methyl Ester Product for Each Cycle			Total of Methyl Ester Percentage
	First	Second	Third	
Cu-BDC	30,26%	28,63%	23,48%	82,37%
Cu-BTC	42,67%	41,72%	35,35%	119,74%
Cu-MOF-74	26,53%	18,61%	11,97%	57,11%
CuMg-MOF-74	17,99%	7,67%	3,24%	28,9%

4 Conclusion

The synthesis of WCO-based biodiesel using heterogeneous catalysts with reflux method has been carried out, followed by quantitative analysis based on the change in FFA content, and qualitative analysis using gas chromatography characterization. From the quantitative analysis, the raw material had FFA value of 12.278%, while the biodiesel products had FFA value ranging from 6.982% to 10.883%. The best FFA reduction was carried out by the Cu-BDC catalyst, where the FFA content fell in the range of 7.46% to 8.92%. Qualitative analysis by gas chromatography showed that HKUST-1 catalyst, especially Cu-BTC, produced the highest ester product compared to MOF-74 catalyst at 42.67%. The performance of copper-based MOF heterogeneous catalyst in this research was not as optimal as the synthesis using NaOH homogeneous catalyst. To resolve this issue, two ways were implemented, such as changing the

ratio between WCO and catalyst and utilizing the reproducibility of the same MOF catalyst to be used for three synthesis cycles. For a constant amount of catalyst, the smaller the amount of WCO, the smaller the FFA of the synthesized product. The synthesis of 75% and 50% WCO with Cu-BDC catalyst resulted in FFA content of 5.49% and 4.826%, respectively. Meanwhile, the highest methyl ester product after three synthesis cycles was experienced by HKUST-1 which amounted to 82.37% with Cu-BDC catalyst and 119.74% with Cu-BTC catalyst.

Acknowledgment

The author wishes to thank Muttaqin Ph.D. and Dr. Nila Tanyela Berghuis S.Si., M.Si. as supervisors throughout the author's research and report writing. Also thanks to all the assistants of the Integrated Chemistry Laboratory and Energy and Material Engineering Research Laboratory of Pertamina University who indirectly helped in launching this research.

References

[1] Quah, R. V., Tan, Y. H., Mubarak, N. M., Khalid, M., Abdullah, E. C., & Nolasco-Hipolito, C. (2019). An Overview of Biodiesel Production using Recyclable Biomass and Non-Biomass Derived Magnetic Catalysts. *Journal of Environmental Chemical Engineering*, *7*(4). https://doi.org/10.1016/j.jece.2019.103219

[2] Tang, Z. E., Lim, S., Pang, Y. L., Ong, H. C., & Lee, K. T. (2018). Synthesis of Biomass as Heterogeneous Catalyst for Application in Biodiesel Production: State of the Art and Fundamental Review. In *Renewable and Sustainable Energy Reviews* (Vol. 92, pp. 235–253). Elsevier Ltd. https://doi.org/10.1016/j.rser.2018.04.056

[3] Jayakumar, M., Karmegam, N., Gundupalli, M. P., Bizuneh Gebeyehu, K., Tessema Asfaw, B., Chang, S. W., Ravindran, B., & Kumar Awasthi, M. (2021). Heterogeneous Base Catalysts: Synthesis and Application for Biodiesel Production – A Review. In *Bioresource Technology*, 331. https://doi.org/10.1016/j.biortech.2021.125054

[4] Liu, X., Liu, Z., Wang, R., & Yang, S. (2020). Functionalized Metal-Organic Framework Catalysts for Sustainable Biomass Valorization. In *Advances in Polymer Technology* (Vol. 2020). Hindawi Limited. https://doi.org/10.1155/2020/1201923

[5] Konnerth, H., Matsagar, B. M., Chen, S. S., Prechtl, M. H. G., Shieh, F. K., & Wu, K. C. W. (2020). Metal-Organic Framework (MOF)-Derived Catalysts for Fine Chemical Production. In *Coordination Chemistry Reviews* (Vol. 416). Elsevier B.V. https://doi.org/10.1016/j.ccr.2020.213319

[6] Samaniyan, M., Mirzaei, M., Khajavian, R., Eshtiagh-Hosseini, H., & Streb, C. (2019). Heterogeneous Catalysis by Polyoxometalates in Metal-Organic Frameworks. In *ACS Catalysis*, *9*(11), 10174–10191. https://doi.org/10.1021/acscatal.9b03439

[7] Gheorghe, A., Strudwick, B., Dawson, D. M., Ashbrook, S. E., Woutersen, S., Dubbeldam, D., & Tanase, S. (2020). Synthesis of Chiral MOF-74 Frameworks by Post-Synthetic Modification by Using an Amino Acid. *Chemistry - A European Journal*, *26*(61), 13957–13965. https://doi.org/10.1002/chem.202002293

[8] Gheorghe, A., Imaz, I., Van Der Vlugt, J. I., Maspoch, D., & Tanase, S. (2019). Tuning the Supramolecular Isomerism of MOF-74 by Controlling the Synthesis Conditions. *Dalton Transactions*, *48*(27), 10043–10050. https://doi.org/10.1039/c9dt01572h

[9] Calleja, G., Sanz, R., Orcajo, G., Briones, D., Leo, P., & Martínez, F. (2014). Copper-Based MOF-74 Material as Effective Acid Catalyst in Friedel-Crafts Acylation of Anisole. *Catalysis Today*, 227, 130–137. https://doi.org/10.1016/j.cattod.2013.11.062

[10] Flores, J. G., Aguilar-Pliego, J., Martin-Guaregua, N., Ibarra, I. A., & Sanchez-Sanchez, M. (2022). Room-Temperature Prepared Bimetallic Nanocrystalline MOF-74 as Catalysts in the Aerobic Oxidation of Cyclohexene. *Catalysis Today*, *394–396*, 295–303. https://doi.org/10.1016/j.cattod.2021.08.025

[11] Jamil, U., Husain Khoja, A., Liaquat, R., Raza Naqvi, S., Nor Nadyaini Wan Omar, W., & Aishah Saidina Amin, N. (2020). Copper and Calcium-Based Metal Organic Framework (MOF) Catalyst for Biodiesel Production from Waste Cooking Oil: A Process Optimization Study. *Energy Conversion and Management*, *215*. https://doi.org/10.1016/j.enconman.2020.112934

[12] Pangestu, T., Kurniawan, Y., Soetaredjo, F. E., Santoso, S. P., Irawaty, W., Yuliana, M., Hartono, S. B., & Ismadji, S. (2019). The Synthesis of Biodiesel using Copper Based Metal-Organic Framework as a Catalyst. *Journal of Environmental Chemical Engineering*, *7*(4). https://doi.org/10.1016/j.jece.2019.103277

[13] Luo, Q. xing, An, B. wen, Ji, M., Park, S. E., Hao, C., & Li, Y. qin. (2015). Metal–Organic Frameworks HKUST-1 as Porous Matrix for Encapsulation of Basic Ionic Liquid Catalyst: Effect of Chemical Behaviour of Ionic Liquid in Solvent. *Journal of Porous Materials*, *22*(1), 247–259. https://doi.org/10.1007/s10934-014-9891-7

[14] Zhang, J., White, G. B., Ryan, M. D., Hunt, A. J., Katz, M. J., & Labrador, C. (2016). Dihydrolevoglucosenone (Cyrene) as a Green Alternative to N,N-Dimethylformamide(DMF) in MOF Synthesis Supporting Information Placeholder. *ACS Sustainable Chemical Engineering*, 4(12), 7186-7192. doi: 10.1021/acssuschemeng.6b02115.

[15] Majano, G., & Pérez-Ramírez, J. (2013). Scalable Room-Temperature Conversion of Copper(II) Hydroxide into HKUST-1 ($Cu_3(btc)_2$). *Advanced Materials*, *25*(7), 1052–1057. https://doi.org/10.1002/adma.201203664

[16] Kamal, K., Bustam, M. A., Ismail, M., Grekov, D., Shariff, A. M., & Pré, P. (2020). Optimization of Washing Processes in Solvothermal Synthesis of Nickel-Based MOF-74. *Materials*, *13*(12), 1–10. https://doi.org/10.3390/ma13122741

[17] Beamish-Cook, J., Shankland, K., Murray, C. A., & Vaqueiro, P. (2021). Insights into the Mechanochemical Synthesis of MOF-74. *Crystal Growth and Design*, *21*(5), 3047–3055. https://doi.org/10.1021/acs.cgd.1c00213

[18] Voskanyan, A. A., Voskanyan, A. A., Goncharov, V. G., Novendra, N., Guo, X., Navrotsky, A., & Navrotsky, A. (2020). Thermodynamics Drives the Stability of the MOF-74 Family in Water. *ACS Omega*, *5*(22), 13158–13163. https://doi.org/10.1021/acsomega.0c01189

[19] Bae, Y. S., Yazayd'n, A. Ö., & Snurr, R. Q. (2010). Evaluation of the BET Method for Determining Surface Areas of MOFs and Zeolites that Contain Ultra-Micropores. *Langmuir*, *26*(8), 5475–5483. https://doi.org/10.1021/la100449z

[20] Feng, L., Wang, K. Y., Willman, J., & Zhou, H. C. (2020). Hierarchy in Metal-Organic Frameworks. *ACS Central Science*, *6*(3), 359–367. https://doi.org/10.1021/acscentsci.0c00158

[21] Zhou, H. C. J., & Kitagawa, S. (2014). Metal-Organic Frameworks (MOFs). In *Chemical Society Reviews* (Vol. 43, Issue 16, pp. 5415–5418). Royal Society of Chemistry. https://doi.org/10.1039/c4cs90059f

[22] Tao, L., Lin, C. Y., Dou, S., Feng, S., Chen, D., Liu, D., Huo, J., Xia, Z., & Wang, S. (2017). Creating Coordinatively Unsaturated Metal Sites in Metal-Organic-Frameworks as Efficient Electrocatalysts for the Oxygen Evolution Reaction: Insights into the Active Centers. *Nano Energy*, *41*, 417–425. https://doi.org/10.1016/j.nanoen.2017.09.055

[23] Ling, J., Zhou, A., Wang, W., Jia, X., Ma, M., & Li, Y. (2022). One-Pot Method Synthesis of Bimetallic MgCu-MOF-74 and Its CO2Adsorption under Visible Light. *ACS Omega*, *7*(23), 19920–19929. https://doi.org/10.1021/acsomega.2c01717

[24] Bagheri, A. R., & Ghaedi, M. (2020). Application of Cu-Based Metal-Organic Framework (Cu-BDC) as a Sorbent for Dispersive Solid-Phase Extraction of Gallic Acid from Orange Juice Samples using HPLC-UV Method. *Arabian Journal of Chemistry*, *13*(5), 5218–5228. https://doi.org/10.1016/j.arabjc.2020.02.020

[25] Stolar, T., Prašnikar, A., Martinez, V., Karadeniz, B., Bjelić, A., Mali, G., Friščić, T., Likozar, B., & Užarević, K. (2021). Scalable Mechanochemical Amorphization of Bimetallic MOF-74 Catalyst for Selective Hydrogenation of CO_2 to Methanol. *ACS Applied Materials & Interfaces*, *13*(2), 3070–3077. doi: 10.1021/acsami.0c21265.

[26] Crawford, S. E., Kim, K. J., Yu, Y., & Ohodnicki, P. R. (2018). Rapid, Selective, Ambient Growth and Optimization of Copper Benzene-1,3,5-Tricarboxylate (Cu-BTC) Metal-Organic Framework Thin Films on a Conductive Metal Oxide. *Crystal Growth and Design*, *18*(5), 2924–2931. https://doi.org/10.1021/acs.cgd.8b00016

[27] Yang, Y., Shukla, P., Wang, S., Rudolph, V., Chen, X. M., & Zhu, Z. (2013). Significant Improvement of Surface Area and CO_2 Adsorption of Cu-BTC via Solvent Exchange Activation. *RSC Advances*, *3*(38), 17065–17072. https://doi.org/10.1039/c3ra42519c

[28] Gupta, J., Agarwal, M., & Dalai, A. K. (2020). An Overview on the Recent Advancements of Sustainable Heterogeneous Catalysts and Prominent Continuous Reactor for Biodiesel Production. *Journal of Industrial and Engineering Chemistry*, 88, 58–77. Korean Society of Industrial Engineering Chemistry. https://doi.org/10.1016/j.jiec.2020.05.012

[29] Gupta, N. K., Kim, S., Bae, J., & Kim, K. S. (2021). Chemisorption of Hydrogen Sulfide over Copper-Based Metal-Organic Frameworks: Methanol and UV-Assisted Regeneration. *RSC Advances*, *11*(9), 4890–4900. https://doi.org/10.1039/d0ra09017d

[30] Britt, D., Furukawa, H., Wang, B., Glover, T. G., & Yaghi, O. M. (2009). Highly Efficient Separation of Carbon Dioxide by a Metal-Organic Framework Replete with Open Metal Sites. *Proceedings of the National Academy of Sciences of the United States of America*, 106(49). doi: 10.1073/pnas.090971810.

[31] Zurrer, T., Wong, K., Horlyck, J., Lovell, E. C., Wright, J., Bedford, N. M., Han, Z., Liang, K., Scott, J., & Amal, R. (2021). Mixed-Metal MOF-74 Templated Catalysts for Efficient Carbon Dioxide Capture and Methanation. *Advanced Functional Materials*, *31*(9). https://doi.org/10.1002/adfm.202007624

[32] Albuquerque, G. H., & Herman, G. S. (2017). Chemically Modulated Microwave-Assisted Synthesis Of MOF-74(Ni) and Preparation Of Metal−Organic Framework-Matrix Based Membranes for Removal of Metal Ions from Aqueous Media. *Crystal Growth and Design*, *17*(1), 156–162. https://doi.org/10.1021/acs.cgd.6b01398

[33] Rong, H., Ji, S., Zhang, J., Wang, D., & Li, Y. (2020). Synthetic Strategies of Supported Atomic Clusters for Heterogeneous Catalysis. In *Nature Communications* (Vol. 11, Issue 1). Nature Research. https://doi.org/10.1038/s41467-020-19571-6

[34] Cirujano, F. G., & Dhakshinamoorthy, A. (2021). Engineering of Active Sites in Metal–Organic Frameworks for Biodiesel Production. In *Advanced Sustainable Systems*, Vol. 5, Issue 8. John Wiley and Sons Inc. https://doi.org/10.1002/adsu.202100101

[35] Dantas, J., Leal, E., Mapossa, A. B., Cornejo, D. R., & Costa, A. C. F. M. (2017). Magnetic Nanocatalysts Of $Ni_{0.5}Zn_{0.5}Fe_2O_4$ Doped with Cu and Performance Evaluation in Transesterification Reaction for Biodiesel Production. *Fuel*, *191*, 463–471. https://doi.org/10.1016/j.fuel.2016.11.107

[36] Naureen, R., Tariq, M., Yusoff, I., Chowdhury, A. J. K., & Ashraf, M. A. (2014). Synthesis, Spectroscopic and Chromatographic Studies of Sunflower Oil Biodiesel using Optimized Base Catalyzed Methanolysis. *Saudi Journal of Biological Sciences*, *22*(3), 332–339. https://doi.org/10.1016/j.sjbs.2014.11.017

[37] Kaisan, M. U., Abubakar, S., Ashok, B., Balasubramanian, D., Narayan, S., Grujic, I., & Stojanovic, N. (2021). Comparative Analyses of Biodiesel Produced from Jatropha and Neem

Seed Oil using a Gas Chromatography–Mass Spectroscopy Technique. *Biofuels*, *12*(7), 757–768. https://doi.org/10.1080/17597269.2018.1537206

[38] Ampairojanawong, R., Boripun, A., Ruankon, S., Suwanasri, T., & Kangsadan, T. (2020). Development of Purification Process Using Electrocoagulation Technique for Biodiesel Produced via Homogeneous Catalyzed Transesterification Process of Refined Palm Oil. *E3S Web of Conferences*, *141*. https://doi.org/10.1051/e3sconf/202014101010

[39] Lawer-Yolar, G., Dawson-Andoh, B., & Atta-Obeng, E. (2021). Synthesis of Biodiesel from Tall Oil Fatty Acids by Homogeneous and Heterogeneous Catalysis. *Sustainable Chemistry*, *2*(1), 206–221. https://doi.org/10.3390/suschem2010012

[40] Viraj Miyuranga, K., Bmcm, B., Thilakarathne, D., SPR Arachchige, U., Weerasekara, N. A., & Jayasinghe, R. A. (2022). Production of Biodiesel Using Acetone as a Co-Solvent. In *International Journal of Scientific Engineering and Science* (Vol. 6, Issue 2). http://ijses.com/

[41] Han, S., & Lah, M. S. (2015). Simple and Efficient Regeneration of MOF-5 and HKUST-1 via Acid-Base Treatment. *Crystal Growth and Design*, *15*(11), 5568–5572. https://doi.org/10.1021/acs.cgd.5b01218

[42] Das, A. K., Vemuri, R. S., Kutnyakov, I., McGrail, B. P., & Motkuri, R. K. (2016). An Efficient Synthesis Strategy for Metal-Organic Frameworks: Dry-Gel Synthesis of MOF-74 Framework with High Yield and Improved Performance. *Scientific Reports*, *6*. https://doi.org/10.1038/srep28050

[43] Marlinda, L., Al Muttaqii, M., & Roesyadi, A. (2016). Production of Biofuel by Hydrocracking of Cerbera Manghas Oil Using Co-Ni/HZSM-5 Catalyst : Effect of Reaction Temperature. *The Journal of Pure and Applied Chemistry Research*, *5*(3), 189–195. https://doi.org/10.21776/ub.jpacr.2016.005.03.254

[44] Yang, L., & Carreon, M. A. (2019). 9 - Green Deoxygenation of Fatty Acids to Transport Fuels over Metal-Organic Frameworks as Catalysts and Catalytic Supports. In *Metal-Organic Frameworks (MOFs) for Environmental Applications* (pp. 285–318). Elsevier. https://doi.org/10.1016/B978-0-12-814633-0.00004-1